Erschienen in: RNA Biology ; 14 (2017), 11. - S. 1522-1533
https://dx.doi.org/10.1080/15476286.2016.1240141

RESEARCH PAPER

The 3′-untranslated region of mRNAs as a site for ribozyme cleavage-dependent processing and control in bacteria

Michele Felletti[a,b], Anna Bieber[a], and Jörg S. Hartig[a,b]

[a]Department of Chemistry, University of Konstanz, Konstanz, Germany; [b]Konstanz Research School Chemical Biology (Kors-CB), University of Konstanz, Konstanz, Germany

ABSTRACT

Besides its primary informational role, the sequence of the mRNA (mRNA) including its 5′- and 3′- untranslated regions (UTRs), contains important features that are relevant for post-transcriptional and translational regulation of gene expression. In this work a number of bacterial twister motifs are characterized both *in vitro* and *in vivo*. The analysis of their genetic contexts shows that these motifs have the potential of being transcribed as part of polycistronic mRNAs, thus we suggest the involvement of bacterial twister motifs in the processing of mRNA. Our data show that the ribozyme-mediated cleavage of the bacterial 3′-UTR has major effects on gene expression. While the observed effects correlate weakly with the kinetic parameters of the ribozymes, they show dependence on motif-specific structural features and on mRNA stabilization properties of the secondary structures that remain on the 3′-UTR after ribozyme cleavage. Using these principles, novel artificial twister-based riboswitches are developed that exert their activity via ligand-dependent cleavage of the 3′-UTR and the removal of the protective intrinsic terminator. Our results provide insights into possible biological functions of these recently discovered and widespread catalytic RNA motifs and offer new tools for applications in biotechnology, synthetic biology and metabolic engineering.

KEYWORDS

Aptazyme; bacteria; hammerhead ribozyme; polyadenylation; riboswitch; RNase; RNA decay; secondary structure; twister ribozyme

Introduction

The function of the mRNA (mRNA) is primarily informational, however, its protein coding sequence (open reading frame, ORF) and its 5′- and 3′-untranslated regions (UTRs) present many features that can modulate gene expression at the transcriptional, post-transcriptional and translational levels.[1,2] In bacteria the 3′-UTR contains the sequence for transcription termination, which can be mediated by either rho-dependent or rho-independent (intrinsic) terminators.[3] The latter consists of a stable hairpin followed by U-rich regions.[4] During rho-independent termination the presence of a weak U-rich RNA:DNA duplex in combination with the formation of a stable RNA hairpin inside the RNA polymerase (RNAP) results in the dissociation of the enzyme from the DNA template and in the release of the mRNA.[3,5,6] In addition to the role in transcription termination, the presence of the intrinsic terminator stem-loop structure is thought to protect the mRNA from the attack of 3′-exonucleases RNase II, RNase R and polynucleotide phosphorylase (PNPase).[7] Protective intramolecular base pairing can also originate as the result of exonucleolytic trimming from an unpaired 3′ end.[8] Interestingly, mRNA degradation initiation from the 3′ end was proposed to become relevant when the target mRNA does not present intrinsic RNase E cleavage sites or when mRNAs or 3′-structured degradation intermediates accumulate abnormally.[7,9,10] In these situations, polyadenylation of the 3′-UTRs, which was shown to favor the degradation of mRNAs, seems to play an important role.[10,11]

Protective RNA structures in the intergenic regions of polycistronic transcripts that are processed by RNase-mediated cleavage can play an important role in the stabilization of the secondary transcripts originating after mRNA processing. For example, Keasling and co-workers showed that the insertion of DNA cassettes containing an RNase E cleavage site and different types of secondary structures could be used to tune the expression of the genes contained in an artificial polycistronic mRNA by regulating the stability of the secondary transcripts generated upon RNase E cleavage.[12-14]

The differential stability of secondary transcripts might be a common mechanism used by bacteria to differentially regulate the levels of expression of genes encoded by the same polycistronic mRNA.[15,16] Processing of mRNAs can also result in the generation of regulatory small RNAs (sRNA). For example, it was shown that the 3′-UTR regions of mRNA transcripts are a large reservoir for Hfq-dependent sRNAs in bacteria.[17] In addition to RNases, small self-cleaving ribozymes were also suggested to be involved in mRNA processing in bacteria and phages.[18,19] In particular, *in vitro* and *in vivo* evidences of hammerhead ribozyme (HHR) mediated cleavage of polycistronic mRNAs in bacteria were reported previously.[18,20]

A genetic context similar to the one observed for HHRs was described for some of the reported bacterial twister ribozymes.[21,22]

CONTACT Jörg S. Hartig joerg.hartig@uni-konstanz.de Konstanz Research School Chemical Biology (Kors-CB), University of Konstanz, 78457 Konstanz, Germany.

This widespread motif shows a high variability in terms of secondary structure. It consists of a catalytic core composed of three stems (P1, P2, and P4) and two pseudoknots (Pk1 and Pk2). While the length of the stems P2 and P4 are rather conserved, stem P1 shows certain variability in length of the stem and of the loop. Additional non-conserved stem-loop structures (P0, P3, and P5) are present in some twister motifs. Three circular permutated configurations are reported (Type P1, P3, and P5), with bacterial representatives in the type P1 and P5 categories. Type P3 contains only motifs found in metagenomes.[21] In a previous work we used a type P3 twister motif for engineering synthetic ligand-dependent RNA switches that regulate the accessibility of the ribosome-binding site (RBS) in the 5′-UTR.[23] These twister-based switches were generated by attaching aptamer sequences to the ribozyme core and by screening for optimized communication modules.

Since it was reported that the twister ribozyme and similar small self-cleaving motifs are frequently found in intergenic region of polycistronic mRNAs, we decided to investigate the influence of ribozyme cleavage on gene expression. In the present work we focus on the influence of ribozyme cleavage in the 3′-UTR, an issue that has received very little attention so far. We characterize several bacterial twister motifs for their potential to influence gene expression in the 3′-UTR. We provide evidence of the possible involvement of these motifs in the processing of mRNAs, proposing the bacterial 3′-UTR as a possible target for cleavage-mediated processing and regulation events. Furthermore, we apply these findings for the development of novel artificial twister-based riboswitches that exert their switching activity via ligand-dependent cleavage of the 3′-UTR. To our knowledge there is only a single short report demonstrating that a theophylline-dependent HHR can be employed in the 3′-UTR of an *E. coli* expression system in order to control gene expression.[24] Our experiments provide insights into possible biological functions of these interesting catalytically active motifs and offer new possibilities for applications in biotechnology, synthetic biology and metabolic engineering.

Results

The ribozyme motifs and their natural genetic contexts

In this study we employed six natural twister motifs features that were identified recently by Breaker and coworkers in bacterial genomes.[21] The selected motifs originate from six different bacterial species: five from *Clostridia* family and one from the *Planctomycetes* phylum. We chose three representatives of the type P1 format and three of the type P5 format, each presenting different structural features. The sequence, the predicted secondary structures, and the genetic contexts of the chosen motifs are shown in Fig. 1. Cbo-2-1 is a phage-associated type P1 twister motif that was found in the genome of *Clostridium botulinum*. It contains a short P3 stem-loop structure and it is located in an intergenic region between the fourth and the fifth gene of a prophage. Interestingly, the ribozyme is found at a point of inversion of the orientation of the phage genes: the first four genes (an integrase, a phage regulatory protein, a transcription regulator and a hypothetical protein) are encoded on the (−) strand, whereas Cbo-2-1 and all other phage genes are encoded on the (+) strand. The ribozyme is

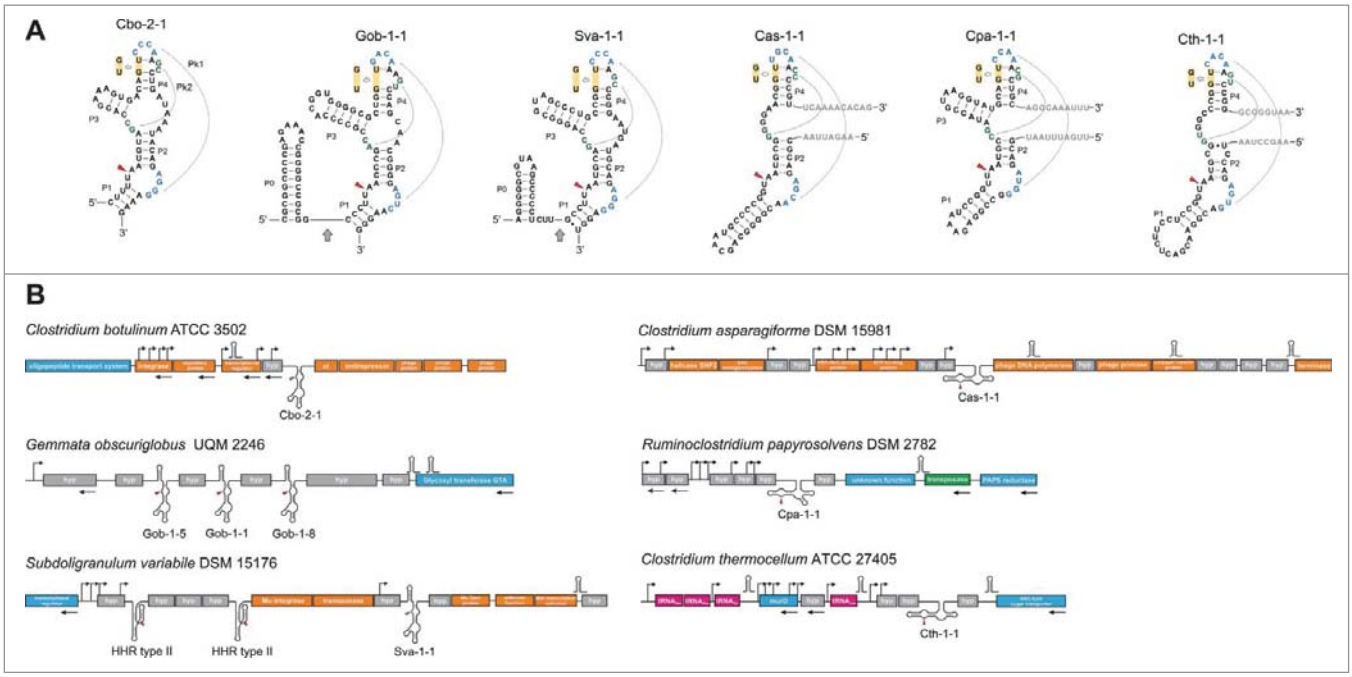

Figure 1. Secondary structures and natural genetic contexts of the twister ribozyme motifs. (A) Pseudoknots Pk1 and Pk2 are highlighted in green and blue, respectively. The inactivating mutation is highlighted in yellow. The cleavage site is indicated with a red arrowhead. The constructs Gob-1-1_w/o_P0 and Sva-1-1_w/o_P0 were generated removing the P0 stem at the position indicated by the gray arrow. The flanking sequences of the 3 type P5 motifs are shown in light gray and were employed in the *in vivo* assay. (B) Natural genetic context of the 6 investigated twister motifs. Genes of phage and bacterial origin are represented in orange and blue, respectively. Transposase, tRNA and hypothetical genes are represented in green, magenta and gray, respectively. Genes with the opposite orientation, whose coding sequence is present on the (-) strand, are indicated with an arrow. The putative promoters (scores between 0.95 and 1.00) are represented with a cornered arrow and putative intrinsic terminators are represented with a hairpin (for details see Table S1 and S2). The only promoter identified in proximity of the Gob motifs has a score of 0.88.

presumably located in the 5′-UTR of a polycistronic transcript where the first open reading frame (ORF) encodes for the phage repressor protein cI, an important regulator of the phage cycle. Different putative promoters were found upstream of the twister ribozyme (Fig. 1B and Table S1 and S2). No intrinsic terminators were identified in the proximity of the ribozyme motif.

Gob-1-1 is one of the eight type P1 twister motifs found in the genome of the planctomycete *Gemmata obscuriglobus*. It presents both a P3 and a P0 stem that are 6 and 10 base pairs (bp) long respectively. Gob-1-1 is surrounded by hypothetical genes. The search for promoters and terminators suggested that it is transcribed as a part of a polycistronic mRNA where two more twister motifs are present (Gob-1-5 and Gob-1-8). Although the sequence of these three motifs is slightly different, they all contain stable GC-rich P0 and P3 stems. Each of the three motifs is located in one of the intergenic regions between the first four genes of the polycistronic mRNA (Fig. 1B). A similar organization is found in two further genetic loci of *G. obscuriglobus*.[21]

Sva-1-1 is one of the two type P1 twister motifs identified in the genome of the anaerobic Gram-negative bacterium *Subdoligranulum variabile*. Similarly to Gob-1-1 it presents both P3 and P0 stem-loop structures, respectively 5 and 7 bp long respectively. Sva-1-1 is found in close proximity of hypothetical and Mu phage genes. The upstream genes include a phage integrase and a transposase. The P0 loop of Sva-1-1 contains the stop codon (UAA) of the upstream ORF encoding for a hypothetical protein. In the downstream region 2 ORFs were assigned to the Gam protein and to the Mor transcriptional activator. The search for promoters and terminators in the proximity of the catalytic motif shows that it has the potential of being transcribed in a long polycistronic mRNA including also two type II hammerhead ribozymes (HHR) (Fig. 1B).

Cas-1-1 is a type P5 twister motif found in *Clostridium asparagiforme*. Similarly to the other P5 motifs, it does not possess an actual P5 stem, but it is directly inserted into the corresponding transcript in correspondence of the site where a P5 stem occurs in type P1 and P3 twister motifs. Moreover, the secondary structure of Cas-1-1 presents a long GC-rich P1 stem-loop. In its natural context it is also associated with phage genes. The catalytic motif is found in the intergenic region between a hypothetical gene and the phage DNA polymerase. The search for promoters resulted in the identification of many possible candidates, some of which are shown in Fig. 1B. The motif can be transcribed potentially as part of a polycistronic mRNA.

Cpa-1-1 is a type P5 twister found in *Ruminoclostridium papyrosolvens*. The predicted secondary structure presents a P3 helix that is 4 bp long. The presence of putative promoters and a terminator suggests that the motif could be transcribed in a polycistronic mRNA. The motif is located in the intergenic region between two hypothetical genes (Fig. 1B).

Cth-1-1 is a type P5 twister ribozyme identified in the genome of *Clostridium thermocellum*. It seems to have a partially degenerated sequence in that the pseudoknot 2 (Pk2) involves two non-canonical GU base pairs and the conserved stem P2 presents a bulge due to the presence of a CC mismatch. The promoter and terminator search shows that it might be transcribed as a part of a polycistronic mRNA, in the intergenic region between two hypothetical genes. tRNA genes are found in close proximity (Fig. 1B).

In vitro characterization of the twister motifs

^{32}P-internally labeled twister motifs where generated by *in vitro* transcription utilizing a blocking strand in order to prevent co-transcriptional cleavage and after purification were characterized in an *in cis* cleavage assay. To evaluate if the P0 stems influence the cleavage of Gob-1-1 and Sva-1-1, 2 additional constructs that lack these stems were generated (Gob-1-1_w/o_P0 and Sva-1-1_w/o_P0, respectively – Fig. 1A). The reaction was started manually with the addition of Mg^{2+} to a final concentration of 1 mM. Magnesium ions were shown to strongly enhance and support the cleavage activity of the twister ribozyme even though they are thought not to be directly involved in the cleavage mechanism.[21,25] A control reaction was analyzed in which 1 mM EDTA was added instead of Mg^{2+} (Fig. S1). Although the *in vitro* transcription was performed in the presence of a blocking strand and the purification of the transcription products was performed in conditions that minimize the presence of divalent cations, a fraction of the ribozymes were already cleaved before the addition of Mg^{2+} in all samples of catalytically active sequences (Fig. 2). Cth-1-1 was catalytically inactive in all tested conditions (Fig. S1H). The obtained time courses were first fitted using the following mono-exponential function (Fig. 2):

$$y = A\, e^{-k_{obst}} + y_0 \quad (1)$$

where k_{obs} is the rate constant of the catalyzed cleavage reaction, y_0 is the final fraction of cleaved RNA and A is the amplitude of the exponential function.

The kinetics of Gob-1-1, Gob-1-1_w/o_P0, Sva-1-1 and Sva-1-1_w/o_P0 were additionally fitted using a bi-exponential function as well (Fig. 2):

$$y = A_1 e^{-k_{1obst}} + A_2\, e^{-k_{2obst}} + y_0 \quad (2)$$

The kinetic parameters and the coefficients of determination (R^2) for each fit are summarized in Tables 1 and 2. The mono-exponential fit resulted to be of good quality for all the analyzed samples, with generally high coefficients of determination (R^2, Table 1). The use of a double exponential function improved the R^2 for Gob-1-1 and Sva-1-1 constructs, however, the standard errors calculated for each of the fit parameters often increased considerably (Table 2). From a qualitative point of view, the double exponential function seems to fit the later data points of the cleavage reaction better (Fig. S2). The fit for the other analyzed motifs using a double exponential function was not possible because it did not converge. It is important to mention that the rate constants derived for Sva-1-1 with and without P0 are interpretable only to a limited extent since most of the cleavage already took place prior to the start of the reaction. This is indicative of a substantial catalytic activity of the ribozyme also in the absence or at low concentrations of

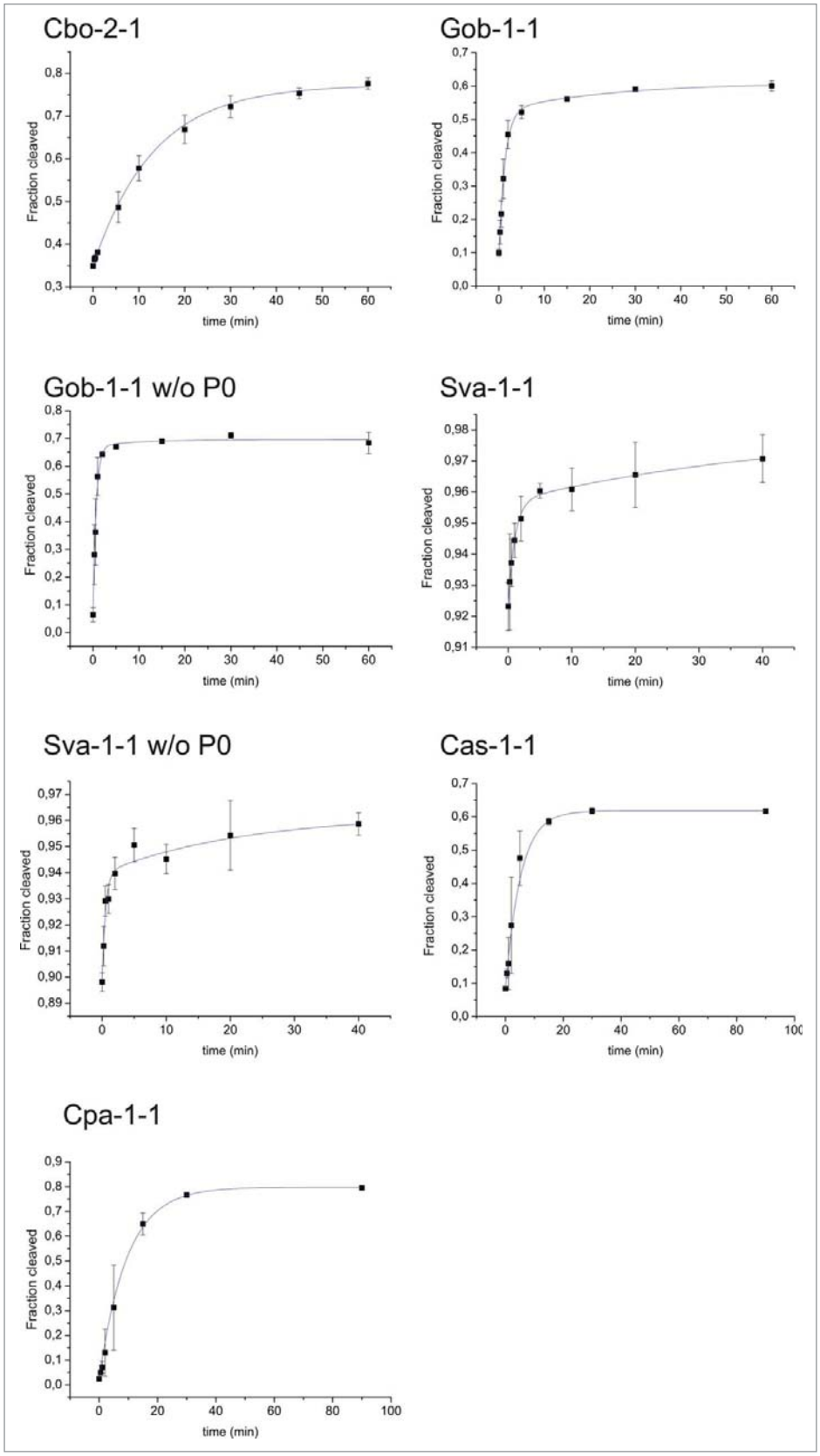

Figure 2. Kinetics of the investigated twister motifs. The kinetics were determined in 50 mM Tris-HCl pH 7.5, 0.1M KCl and 1 mM $MgCl_2$. The kinetic traces were fitted with either mono exponential (Cbo-2-1, Cas-1-1 and Cpa-1-1) or double exponential functions (Gob-1-1, Gob-1-1 w/o P0, Sva-1-1 and Sva-1-1 w/o P0). The error bars represent the standard deviations calculated on independent triplicates. The relative kinetic parameters are reported in Table 1 and Table 2. Representative PAGE images of the kinetics and of the EDTA controls are reported in Fig. S1.

Table 1. Fitting parameters of the kinetics traces using a mono-exponential function. k_{obs} is the rate constant of the catalyzed cleavage reaction, y_0 is the final fraction of cleaved RNA and A is the amplitude of exponential function. R^2 is the coefficient of determination of the fitting. The errors relative to the fitting parameters are reported as standard errors (σ). Note that the Cth-1-1 motif was inactive.

	k_{obs} (min^{-1})	σ_{kobs} (min^{-1})	A	σ_A	y_0	σ_{y0}	R^2
Cbo-2-1	0.075	0.004	−0.422	0.005	0.773	0.006	0.999
Gob-1-1	0.525	0.118	−0.476	0.017	0.577	0.007	0.99
Gob-1-1 w/o P0	1.295	0.116	−0.624	0.031	0.689	0.006	0.981
Sva-1-1	0.612	0.148	−0.037	0.003	0.963	0.002	0.948
Sva-1-1 w/o P0	1.021	0.271	−0.053	0.005	0.952	0.003	0.935
Cas-1-1	0.191	0.008	−0.534	0.002	0.618	0.002	0.999
Cpa-1-1	0.105	0.006	−0.773	0.005	0.798	0.005	0.999

bivalent ions. Regarding the effects of the presence of a P0 stem-loop, we noted that the observed cleavage rate constants were generally higher for constructs without P0, indicating that the presence of a P0 stem at the base of P1 slightly inhibits the cleavage rate of the ribozyme. Two-state kinetics were observed for both constructs with and without the P0 stem.

Influence of twister motifs on gene expression

To investigate how the cleavage of the 3′-UTR of a reporter gene by the different motifs can influence gene expression *in vivo*, catalytically active and inactive forms of the different twister motifs were inserted between the stop codon and the intrinsic terminator stem of an eGFP gene contained in the pET16b plasmid in *E. coli*. The catalytically inactive forms of the twister ribozymes were generate by inverting the order of two conserved nucleotides (nt) in the stem P4 as proposed by Roth et al.[21] The eGFP reporter gene is expressed under the control of a T7 promoter that is leaky with regard to IPTG induction.[23]

The levels of eGFP expression were compared with a positive control composed of an unstructured 3′-UTR between the stop codon and the terminator stem-loop structure (Fig. 3A, B). Due to the fact that the three selected type P5 twister motifs do not possess actual P5 stems, the ribozymes were inserted into the 3′-UTR including their natural flanking sequences (light gray in Fig. 1A). The length of these flanking sequences was 8 nucleotides on both ends for Cth-1-1, 10 nt on both ends for Cpa-1-1 and 8 nt at the 5′ end and 11 nt at the 3′ end of Cas-1-1. Moreover, to evaluate the effect of the presence of the P0 stems in Gob-1-1 and Sva-1-1, two additional constructs were tested where these secondary structures are missing. The clones were let outgrow overnight in LB medium. Bulk fluorescence measurements were used to evaluate the levels of eGFP expression in the stationary phase. The data were normalized against OD_{600}, and the bulk fluorescence values of the active and inactive constructs were compared. The results are shown in Fig. 3C. While the level of eGFP expression remains in a range similar to the positive control when a catalytically inactive ribozyme is inserted into the 3′-UTR, a decreased eGFP expression is observed for all clones carrying an active ribozyme sequence, with the notable exception of the Cth-1-1 construct that proved catalytically inactive in the *in vitro* cleavage assays. The reporter gene expression decreases to different extents in the different active constructs when compared to the positive and to the catalytically inactive controls: the observed effect is very pronounced for Cpa-1-1 (type P5). Cbo-2-1, Gob-1-1 lacking P0 stem and both Sva-1-1 constructs (type P1). The effect is weak in the type P5 Cas-1-1 and in the Gob-1-1 motif with P0 stem. These experiments demonstrate that ribozyme cleavage in the 3′-UTR significantly affects gene expression. In addition, our data show that the stem-loop P0 often found in the natural context has a significant influence on gene expression in the Gob-1-1 construct: when it is present, the eGFP expression decreases less then in the construct without P0. This effect is also visible but less pronounced in the Sva-1-1 construct. Next, we performed a correlation analysis to investigate the relation between the kinetic parameters determined by *in vitro* cleavage assays and the levels of eGFP expression observed in the different active constructs. For the analysis we used the kinetic parameters derived from the mono-exponential fit because they are characterized by a lower standard error. In Fig. 3D the eGFP expression levels of each twister construct are plotted against the relative k_{obs} and y_0 values (Table 1). Pearson correlation coefficients were calculated showing a very weak correlation between the eGFP expression levels due to the insertion of a twister ribozyme into the 3′-UTR of the reporter gene, and the k_{obs} of the motif ($\rho = 0.248$ p-value = 0.5915). Interestingly, a moderate and statistically significant negative linear correlation was observed between y_0, the final total fraction of cleaved ribozyme, and the eGFP expression level ($\rho = 0.754$ p-value = 0.0502). As a tendency, this suggests that ribozymes displaying a higher final cleaved RNA fraction in the *in vitro* assay show lower levels of eGFP expression in the *in vivo* assay. The absence of a strong correlation between the *in vitro* determined kinetic parameters and the levels of reporter gene

Table 2. Fitting parameters of the kinetic traces using a double-exponential function for some of the twister motifs. k_{1obs} and k_{2obs} are the rate constants of the 2 kinetic processes, y_0 is the final fraction of cleaved RNA and A_1 and A_2 are the amplitudes of the 2 exponential functions. R^2 is the coefficient of determination of the fitting. The errors relative to the fitting parameters are reported as standard errors (σ).

	k_{1obs} (min^{-1})	σ_{k1obs} (min^{-1})	k_{2obs} (min^{-1})	σ_{k2obs} (min^{-1})	A_1	σ_{A1}	A_2	σ_{A2}	y_0	σ_{y0}	R^2
Gob-1-1	0.754	0.114	0.042	0.055	−0.438	0.036	−0.085	0.0329	0.61	0.035	0.993
Gob-1-1 w/o P0	1.461	0.23	0.103	0.59	−0.607	0.066	−0.025	0.061	0.696	0.027	0.995
Sva-1-1	0.932	0.123	0.022	0.029	−0.033	0.002	−0.023	0.016	0.98	0.018	0.995
Sva-1-1 w/o P0	1.879	0.78	0.045	0.092	−0.042	0.008	−0.022	0.012	0.962	0.016	0.964

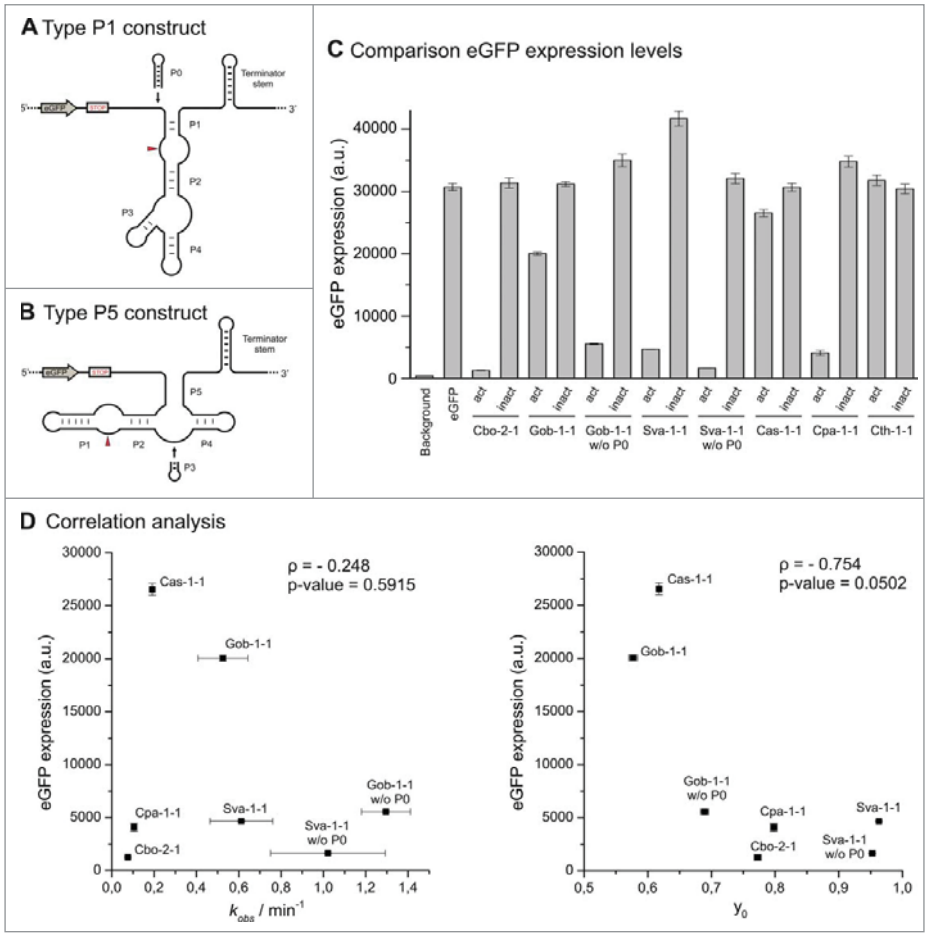

Figure 3. Gene expression assay and correlation analysis. (A) The general design of the reporter type P1 and type P5 constructs. The cleavage site is shown by a red arrowhead. (B) eGFP expression levels of the catalytically active and inactive twister constructs inserted into the eGFP 3′-UTR. Error bars represent standard deviations calculated on independent biological quadruplicates. (C) Scatter plots of the levels of eGFP expression of the active twister constructs against the observed cleavage rate constant k_{obs} (left panel) and the final fraction of cleaved RNA y_0 (right panel) for each motif. The error bars represent standard deviations derived from the fit with equation (1). Correlation coefficients and p-values were calculated for both data sets.

expression suggests that other factors such as the ribozyme format and the presence of specific structural features could influence the extent of gene expression. However, more twister motif sequences that differ in formats and structural features need to be studied in order to better understand the factors that determine the impact of twister ribozyme cleavage on gene expression in the 3′-UTR. Apart from gaining insight into structure-function relationships the investigation of the influence of twister cleavage of the 3′-UTR was motivated by an interest to use this motif in the 3′-UTR for constructing artificial genetic switches.

Twister-based artificial riboswitches in the 3′-UTR

In order to test the possibility of modulating the catalytic activity of a self-cleaving ribozyme inserted into the 3′-UTR of a transcript for achieving external regulation of gene expression, we generated ligand-dependent ribozymes (aptazymes) that can control gene expression via direct cleavage of the 3′-UTR of the reporter. Here, aptazymes are used as a model of direct regulation of the cleavage activity catalytic motif, simulating *in vivo* the control of a ribozyme by a protein factor, or a cellular metabolite. To do so, we employed a type P3 twister ribozyme (env-9) derived from an environmental sequence (Fig. 4A) that has been already used with success for RNA engineering purposes in *E. coli* and yeast.[23] Although the kinetic features have been extensively described by Breaker and coworkers,[21] its genetic context remains uncharacterized and it is difficult to make hypotheses regarding its biological function. Previously we demonstrated that this twister motif is very well suited as a flexible and modular expression platform for the development of artificial riboswitches that rely on the masking of the RBS in the 5′-UTR for controlling gene expression.[23] For this reason we decided to use this motif to engineer novel twister-based switches for the 3′-UTR.

We first tested the *in vivo* activity of an engineered env-9 with a shortened P1 stem to avoid secondary effects due to the presence long and stable secondary structure in the 3′-UTR upon cleavage (Fig. 4B), comparing the eGFP expression levels of the catalytically active and inactive 3′-UTR constructs. The cleavage of the 3′-UTR promoted by this motif significantly decreased eGFP expression when compared with the positive control and with the catalytically inactive control (Fig. 4D, E). In order to develop ligand-dependent twister ribozymes active in the 3′-UTR, we first tested aptazyme sequences that were developed for the use in the 5′-UTR. In particular, we employed twister-based theophylline and thiamine pyrophosphate (TPP) aptazymes that were presented in our previous work using a

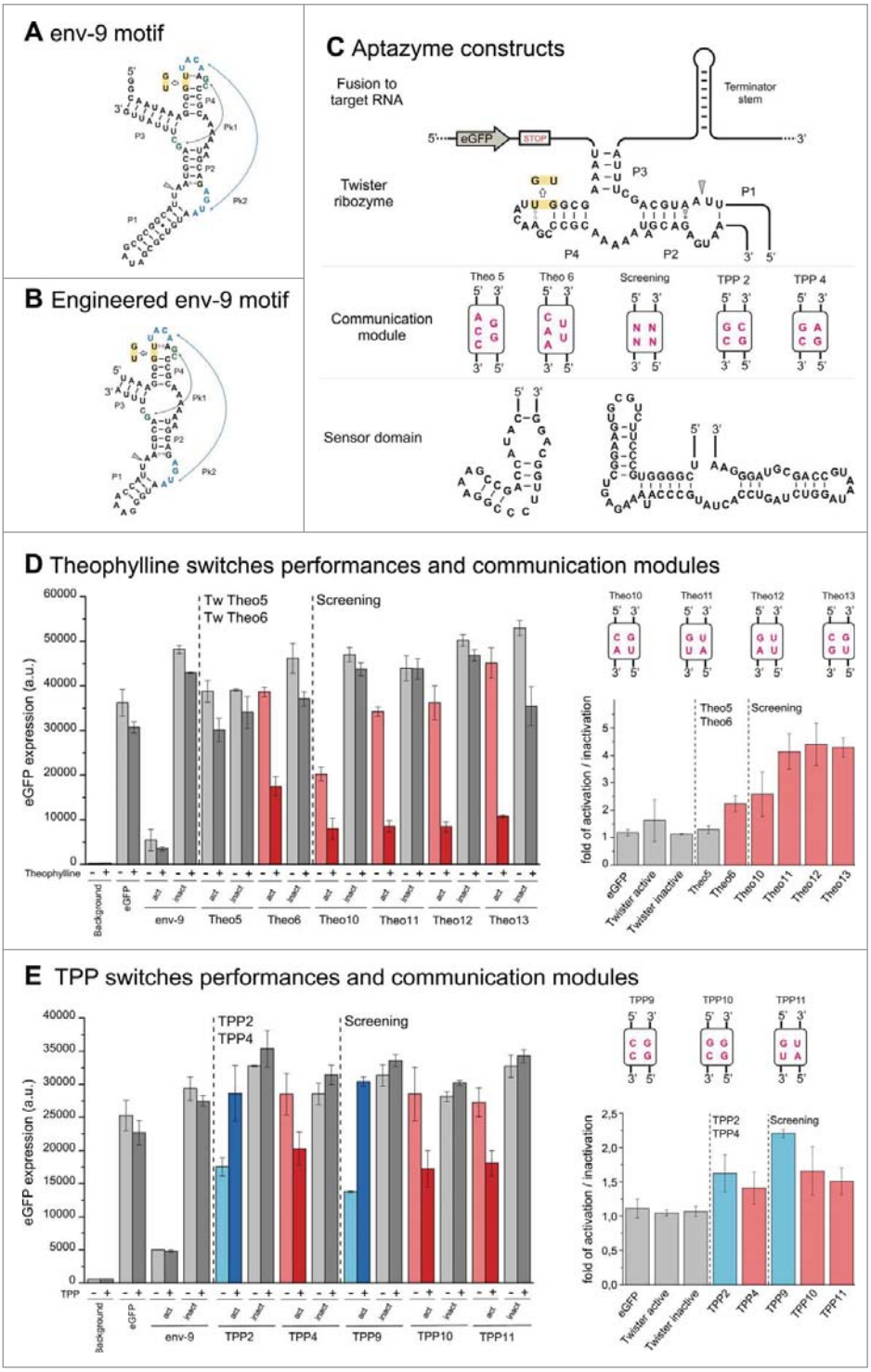

Figure 4. Design and performances of the artificial riboswitches in the 3′-UTR. The twister-based artificial riboswitches based on the naturally occurring env-9 motif (A) with shortened P1 and P3 stems (B). Theophylline and TPP aptazymes were generated connecting 2 aptamer domains to the stem P1 of the catalytic motif (C). Previously isolated communication modules were employed (Theo 5, Theo 6, TPP 2 and TPP 4). In addition 2 combinatorial libraries were generated using communication modules of 4 randomized nucleotides. The inactivating mutation is highlighted in yellow. The cleavage site is indicated by an arrowhead. (D,E) left panel: eGFP expression (bulk fluorescence divided by the relative OD_{600}) of the selected active and inactive clones in the absence (−) and presence (+) of (D) 2.5 mM theophylline and (E) 1 mM thiamin in the culture medium. Right panel, the performances (fold of activation or inactivation) of the on- and off-switches were calculated as the ratio of fluorescence of active divided by inactive expression states using background subtraction. The levels of reporter gene expression in the different conditions are represented by gray (controls), red (off-switches) and blue bars (on-switches). Error bars represent standard deviation calculated from independent biological triplicates. The identified communication modules are reported. Note that the numbering of the switches was assigned to be consistent with previously identified communication modules for twister-based theophylline and TPP switches in the 5′-UTR.[23]

SD masking strategy (Theo5, Theo6, TPP2 and TPP4 – Fig. 4C). These aptazymes present either a theophylline or a TPP aptamer connected to the stem P1 of the catalytic domain through a communication module that was isolated upon *in vivo* screening. Theo5 and TPP2 are inactivated by the presence of the ligand. In the 5′-UTR, this results in the masking of the

SD sequence and in the down-regulation of eGFP expression (off-switch). In the 3′-UTR the inactivation of the catalytic activity due to the presence of the ligand in the culture medium is expected instead of the up-regulation of gene expression (on-switch). In an analogous way, Theo6 and TPP4 aptazymes are activated by the presence of the ligand and in our design in the 5′-UTR this results in the upregulation of the expression (on-switch). In the 3′-UTR the presence of the ligand is expected to induce downregulation of gene expression (off-switch). Our data show that Theo5 does not have any switching activity when inserted into the 3′-UTR, whereas Theo6 seems to have a weak off-switch activity (about 2-fold) (Fig. 4D). TPP2 and TPP4 show the expected behavior in the 3′-UTR, even though switching performances are very weak (only 1.5-fold) (Fig. 4E). In order to improve twister-based aptazyme switches for the 3′-UTR we applied an *in vivo* screening approach. Two aptazyme combinatorial libraries were generated connecting two different aptamers (theophylline and TPP) to the stem P1 of the catalytic domain using a communication module of four randomized nucleotides (Fig. 4C). The stem P1 was chosen because it was shown to be more suited compared to the position P5.[23] The combinatorial libraries were transformed in *E. coli* and single clones were screened for differential expression of eGFP in the presence and in the absence of the respective ligand.

The screening of new communication modules in the 3′-UTR resulted to be more suited for the isolation of effective riboswitches. In fact, seven twister-based switches resulted from the screening. The isolated clones were sequenced and catalytically inactive mutants were generated to verify that the switching activity is dependent on the self-cleavage reaction. In particular, the screening of the theophylline library resulted in the isolation of 4 off-switches that show moderate decrease in fluorescence of up to 4.5-fold upon the addition of theophylline (Fig. 4D). The overall switching activity of the isolated TPP riboswitches in the 3′-UTR was always week, with around 2.2-fold for the on-switch and around 1.8-fold for the two OFF-switches. Consistently with what was previously noticed, the presence of only strong GC Watson-Crick (WC) base pairs in the communication modules is observed mostly in aptazymes that are inactivated by the presence of the ligand (in total four out of five communication modules in P1, including the ones identified in our previous work.[23] On the contrary, the presence of non-WC base pairs or less frequently the presence of AU pairs results in aptazymes that are activated by the presence of the ligand (all the 12 communication modules in P1, including the ones identified in our previous work). Finally, it is interesting to note that in all cases the off-state of the switch is characterized by a relatively high residual eGFP expression, indicating a significant leakiness of these artificial devices.

Discussion

Small endonucleolytic ribozymes have been shown to be present in all domain of life.[18,20,26] The presence of HHRs in the mRNAs of prophages and bacteria was suggested to be involved in the generation of smaller transcripts starting from a long polycistron, in the generation of spliced or circular processed transcripts (via cleavage followed by ligation reaction) or in the generation of sRNAs.[18,19] In particular, Perrault et al. showed that three tandem HHR arrangements generate fragments of the native polycistronic RNA in an *in vitro* transcription assay as well as *in vivo*, after cloning and transcription of the DNA locus in *E. coli*.[18,19] In eukaryotes HHRs were found in intronic sequences, indicating a potential role in pre-mRNA processing,[27] and in non- autonomous retroelements.[28,29] Previously, small Mn^{2+}-dependent ribozymes were identified in the 3′-UTR of *Xenopus laevis* Vg1 and β-actin mRNAs.[30] Although the motif found in the Vg1 mRNA showed Mn^{2+}-dependent self-cleavage *in vitro*, no activity was detected *in vivo*.[30]

A distribution similar to the one of the hammerhead ribozymes was observed also for some of the recently described twister ribozymes.[21] Until now, no defined biological role had been assigned to any of the employed twister ribozyme. This is also due to the fact that the genomic regions and described organisms where the motifs were identified are generally poorly characterized. Many twister ribozyme motifs were noted to be associated with other small self-cleaving ribozymes belonging to the twister class or to other classes.[21,22] Moreover, a common proximity of these ribozymes to a series of conserved protein domains was observed, notably to numerous elements related to Mu bacteriophages.[21,22] All the investigated motifs in this work are located in bacterial genomes. The analysis of the genetic context confirmed the potential for these motifs to be transcribed in intergenic regions as part of polycistronic mRNAs, with the only exception of Cbo-1-1 that seems to be located in the 5′-UTR of the first gene of the transcript. Furthermore, Gob-1-1 and Sva-1-1 seem to be present on the transcript together with other twister and hammerhead self-cleaving motifs. With the exclusion of Cth-1-1 a moderate cleavage activity *in vitro* was observed for all the tested motifs. The cleavage kinetics of Sva-1-1 and Gbo-1-1 can be described with a biphasic behavior. The latter can be explained by the existence of a second, slower (up to 10-fold) process, taking place in addition to the cleavage reaction such as a conformational change of the ribozyme (observed before with some HHR sequences)[31] or the contemporaneous cleavage reaction of two alternative conformations of the ribozyme. The insertion of catalytically active twister motifs into the 3′-UTR resulted in altered gene expression. The effects on gene expression can be explained by the destabilization of the transcript following the RNA cleavage and the consequent removal of the protective intrinsic terminator stem-loop structure. The gene expression levels seem to be only partially dependent on the catalytic characteristics of the motif. We observed a very weak negative correlation of the reporter gene expression levels with the k_{obs} of the motif and a moderate statistical negative correlation with total fraction of cleaved ribozyme (y_0) in the *in vitro* assay. A possible explanation for these results requires taking in consideration the half-life of the eGFP transcript. In *E. coli*, overall mRNA half-lives were reporter to range between 1–15 min in LB medium at 30 °C and 6.8 min at 37 °C.[32,33] The mRNA half-life of an eGFP transcript with a common transcription terminator in *E. coli* was reported to be ~8 min.[12] The resulting mRNA decay rate constant $k_{dec} = ln2 / t_{1/2} \approx 0.087\ min^{-1}$ is smaller than all obtained ribozyme cleavage constants *in vitro* (or comparable in the case of Cbo-2-1). In case that the mRNA has a similar half-life in our system and assuming that the folding of the ribozyme is not rate-limiting, a substantial part of the

mRNA will be cleaved by all tested motifs before the mRNAs is degraded. In bacteria the main 3′-exonucleases involved in bulk mRNA degradation are suggested to be RNase II, RNase R, PNPase and Oligoribonuclease (Orn).[10,34] RNase II and PNPase are both known to stall 6–8 nt before stable G/C-rich secondary structures, whereas RNase R is able to degrade structured substrates, but requires at least 7 nt as single-stranded 3′ overhang.[34] Hence, the removal of the terminator stem-loop from the transcript by the ribozyme results presumably in an overall increased rate of the eGFP mRNA degradation,[7,12,13] thereby reducing the level of transcripts available for translation. Interestingly, the reporter gene utilized in this study was previously reported to be not susceptible to inactivation by RNase E.[12] Hence 3′-exonucleolytic degradation mechanisms might be relevant for *gfp* mRNA stability.

Under these conditions, the effect of the cleavage on the gene expression is expected to be dependent on both the total fraction of the cleavage product y_0 and on the cleavage rate constant. It is important to mention that the destabilization of a transcript can be observed at the level of protein expression only if the translation is limited by the availability of the transcript. If for example many copies of the transcript are present in the cell (due to either high level of transcription or high gene copy number), the availability of ribosomes can become the limiting factor and hence stabilization of the transcript might not result in high protein levels.[13] However, the low correlation factors indicate that the kinetic features of the motifs cannot fully explain the level of reporter gene expression. The difference of gene expression levels observed for the Gob-1-1 and the Sva-1-1 constructs with and without P0 stems indicates that the presence of secondary structures associated with the ribozyme might play a relevant role. As the cleavage site of the ribozyme lies within the loop L1 (Fig. 1A), upon cleavage of Gob-1-1 and Sva-1-1 the P0 stem-loop remains in the 3′-UTR of the reporter. By contrast, no stable secondary structure is remaining in the 3′-UTR in the case of motifs that lack the stem P0. The higher levels of eGFP expression in the catalytically active constructs containing stem P0 compared to the one without the stem-loop might indicate that these structures have a protective role on the mRNA. However, our data indicate that the P0 stem is not able to completely protect the transcript against degradation, especially in the Sva-1-1 construct. The limited effects observed comparing the Sva-1-1 constructs with and without the additional stem could be explained by the fact that the P0 stem in Sva-1-1 is significantly shorter than the one of Gob-1-1. Indeed larger hairpins in the 3′-UTR are expected to have stronger protective effects on the transcript.[14] Moreover, the 8 nt long single stranded stretch region at the 3′ end of the cleaved Sva-1-1 construct could make the mRNA more susceptible to RNase II degradation, which was shown to require at least 7 nt for the degradation of stable secondary structures.[34] Similar protective effects on the processed mRNA can be supposed for large P1 stems in type P5 twister ribozymes that remain in the 3′-UTR upon cleavage. Such an effect could contribute to the difference observed between the Cpa-1-1 construct, which contains a large CG rich P1 stem, and the Cas-1-1 construct, which contains a shorter P1 stem. Interestingly, stem P1 was reported to be not essential for the catalysis of the twister ribozyme,[35] opening the possibility that this structure can have also have regulatory roles. Moreover, it was also shown that transcription terminator stem-loop structures are preferred substrates for polyadenylation by PAPI,[10,36] even though a short single stranded region at the 3′ end is necessary.[37] The addition of poly(A) tails by poly(A) polymerase (PAPI) or polynucleotide tails by PNPase to the 3′ end of structured mRNA facilitate the degradation of structured RNAs by 3′ exonucleases, particularly by RNase R.[7,34,38] Following ribozyme cleavage, the 3′ single stranded regions on the Gob-1-1, Sva-1-1 and Cas-1-1 constructs are 6, 8 and 2 nt long, suggesting a possible correlation with the susceptibility to polyadenylation and the effects observed on gene expression *in vivo*. The Gob-1-1 twister motif studied here is particularly interesting because in its natural genetic context it occurs close proximity to two more twister motifs (Gob-1-5 and Gob-1-8). According to our promoter and terminator search, all three motifs are present on a single polycistronic transcript. The organization of this genetic locus resembles the one observed for some tandem hammerhead arrangements in bacteria.[18] Moreover, a similar tandem organization is observed in two more loci in the same *G. obscuriglobus*.[21] Intriguingly, all 8 twister motifs identified in *G. obscuriglobus* contain a large and stable P0 stem.

This finding suggests a possible protective role of these structures in the secondary transcripts originating upon cleavage. Interestingly, it was already shown that artificial and natural operons can take advantage of RNase-mediated processing to uncouple the expression of the proteins encoded by a polycistronic mRNA. Secondary transcripts originating after RNase cleavage can possess different stabilities due to a variety of factors, including the different secondary structure present in the 5′- and 3′-UTRs. The differential stability of these secondary transcripts resulted to be an efficient mechanism to regulate the relative amounts of the proteins encoded by the polycistron using only one promoter.[12-16] Further discussion regarding potential functions of additional structural features, the advantage and potential problems of studying the twister motifs in *E. coli*, and the use of T7 polymerase instead of the endogenous polymerase can be found in the Supporting Information.

In addition to the demonstration of the effect of twister-mediated cleavage of the 3′-UTR on gene expression levels, we constructed artificial ribozyme-based ligand-dependent switches in the 3′-UTR. In this case the switching mechanism is based on the removal of the stabilizing terminator stem-loop upon cleavage. Using a ribozyme motif that after cleavage does not leave protective secondary structures in the resulting transcript, a ligand-dependent activation of the catalytic motif should result in a decrease in gene expression (off-switch) whereas ligand-dependent inactivation should result in induced gene expression (on-switch), resembling the behavior of ribozyme-based switches of gene expression realized in eukaryotic organisms.[39] Importantly, only off-switches were obtained for theophylline. This is in line with the previously reported HHR- and twister-based switches that in the context of the 5′-UTR only yielded on-reactivity. This can be explained with the ligand binding resulting in a stabilization of the ribozyme fold. Although this design strategy (activation of ribozyme upon ligand binding) limits the applications of the switches, with the present work such switches can still be used to switch off

gene expression in bacteria when they are applied in the 3′-UTR instead of the 5′-UTR. Hence, the concept presented here significantly broadens the repertoire of RNA-based switches for controlling gene expression.

Since switches developed initially for the application in the 5′-UTR performed worse in comparison to switches that were screened in the 3′-UTR context, it seems advantageous to optimize sequences in the desired genetic context. In general, switches engineered using the theophylline aptamer as sensor domain showed better performances compared to the ones obtained using the TPP aptamer. The TPP aptamer in presence of Mg^{2+} adopts a folded structure that presents two stable sensor helix arms (P2/P3 and P4/P5).[40] As in the twister-based TPP switches presented in this work, the aptamer domain remains on the 3′-UTR of the secondary transcript upon cleavage, we can speculate that this structure can have a stabilizing effect analogous to the one of the terminator stem-loop. This would strongly decrease the switching performances because the removal of the terminator stem mediated by the aptazyme (regardless whether positively or negatively regulated by the ligand) would not result in an effective destabilization of the mRNA. The presence of secondary structures in the 3′-UTR upon cleavage seems an important factor to take into consideration for the design of such artificial riboswitches.

In conclusion, we demonstrate that ribozyme-mediated cleavage in the 3′-UTR influences gene expression in bacteria. We provide evidence that the effects on gene expression do not depend primarily on the kinetic characteristics of the ribozyme but mainly on motif-specific structural features. The analysis of the genetic contexts of naturally occurring twister motifs hints at a role of these ribozyme motifs in the processing of bacterial and phage polycistronic transcripts. The ribozyme-mediated cleavage of the primary transcript could generate a number of secondary transcripts that present differential stability and can be differentially translated depending on the secondary structures that are left on the untranslated regions of the secondary transcripts, similarly to observations made for RNase-mediated cleavage.[12,14-16] The suggested model for ribozyme-mediated gene expression modulation in the 3′-UTR should be generally applicable in bacteria, as 3′-exoribonucleolytic degradation is a universal feature in bacteria.[34] We have demonstrated that we can take advantage of ribozyme-mediated cleavage of the 3′-UTR in order to develop artificial ribozyme-based switches in bacteria. The use of ribozymes with different structures and catalytic properties or ligand-dependent ribozymes could be convenient for applications such as metabolic engineering where the expression of artificial operons needs to be coordinated and controlled. The use of ribozymes could represent an alternative to the use of RNase E or CRISPR cleavage sites.[12,14,41]

Material and methods

Promoter and terminator search

The genomic sequences of the 6 bacterial strains carrying the twister motifs were obtained from NCBI nucleotide database (http://www.ncbi.nlm.nih.gov - accession number reported in the Table S1). The promoter and the intrinsic terminator searches were performed in the proximity of the ribozyme motif and on the same DNA strand. The neural network promoter prediction tool specific to bacterial promoters developed in the context Berkeley Drosophila Genome project (www.fruitfly.org/seq_tools/promoter.html) and ARNold tool (http://rna.igmors.upsud.fr/toolbox/arnold/) were employed for the search of putative promoters and terminators respectively. ARNold search procedure uses two programs to find rho-independent terminators: Erpin and RNAmotif.[4,42,43]

Plasmid construction

The twister motifs and the aptazyme motifs (including the library) were inserted into the pET16b_eGFP plasmid by whole-plasmid PCR with Phusion Hot Start 2 Polymerase (NEB) using primer pairs that contained the sequence of the motifs into the 5′ overhang ends. For each pair, one of the primers was 5′ phosphorylated. Catalytically inactive mutants were generated by site-direct mutagenesis PCR using the suitable pET16b_eGFP containing the catalytically active form as template. After PCR, the template plasmid was digested using the enzyme DpnI (NEB). The PCR products were purified by band purification after gel electrophoresis (0.8 % GTQ agarose - Roth). The purified products were blunt end ligated (Quick Ligase, NEB) and transformed into *E. coli* BL21(DE3) gold (Stratagene) by electroporation. The transformed bacteria were plated on Luria-Bertani (LB) agar Petri dishes supplemented with 100 μg per mL carbenicillin and grown aerobically at 37 °C overnight. To confirm successful cloning, the cloned plasmids were isolated (Miniprep Kit, Qiagen) and sequenced (GATC Biotech).

RNA preparation

The different catalytic motifs were obtained by *in vitro* transcription starting from a DNA template, in the presence of DNA blocking strands (~25 nt, melting temperature 70–80 °C). The DNA templates were generated by *Taq*-PCR (NEB) using the suitable pET16b_eGFP containing the catalytically active form of the twister motif as template. The forward primers were designed with the following 5′ overhang that contained a T7 promoter sequence: 5′AAATTAATACGACTC ACTATAGGGAG3′. The total PCR reaction volume was 200 μL. The PCR products were ethanol precipitated (1/10 volume of 3 M sodium acetate pH 5.7 and 3 volumes of 100% ethanol - Sigma-Aldrich). The pellets were resuspended in 40 μL of ddH_2O. The PCR products were *in vitro* transcribed using T7 RNA polymerase (Thermo Scientific) in Thermo Scientific transcription buffer, 90 nM ATP, 2 mM CTP, 2 mM GTP and 2 mM UTP, 80 U RiboLock RNase Inhibitor (Thermo Scientific), 0.15 U of PPase (Thermo Scientific), 5 μCi ^{32}P-α-ATP and in presence of 25 μM blocking strand. Transcription was carried out for 2 hours at 37 °C. Afterwards the reaction mixes were ethanol precipitated overnight and resuspended in 40 μL of ddH_2O. One volume of 2X loading buffer (80% [v/v] formamide, 50 mM EDTA pH = 8.0) was added. Subsequently the products were purified by 8% denaturing PAGE (10% for motifs without P0). Electrophoresis was performed at 600 V, 300 mA, 100 W for 3 h (4.25 h for constructs without P0). Full-

length products were excised and extracted from gel using 500 μL Rotipuran water (Roth) supplemented with 1 mM EDTA at 6 °C, 1400 rpm overnight. All the following steps were performed using Rotipuran water to minimize the presence of divalent cations. The samples were filtered through glass wool and the RNA was ethanol precipitated over night and resuspended. RNA concentrations were determined spectrophotometrically.

In vitro cleavage assay

Activities were determined in 50 mM Tris-HCl pH 7.5, 0.1 M KCl. The final concentration of the RNA in the reaction mix was 180 nM. The folding of the RNA motif was performed incubating the reaction mix at 95 °C for 2 min and then slowly cooling down to 37 °C in the absence of Mg^{2+}. The cleavage reaction was started by manual addition of Mg^{2+} to a final concentration of 1 mM. Reactions were quenched with loading/stop buffer (80% [v/v] formamide, 50 mM EDTA pH = 8.0, 0.025 % [w/v] bromophenol blue and 0,025% [w/v] xylene cyanole) after defined time points. The reactions were peformed in triplicates with one EDTA control (final concentration 1 mM, no $MgCl_2$) for each motif. 2 μL of reaction mix were analyzed by 8% PAGE (80 well analytical gel, 1800 V, 300 mA, 100 W, 1.5 – 2.5 h). The results were visualized by phosphorimaging and the bands were quantified with ImageQuant TL. The fractions of cleaved RNA were calculated for each time point from the intensities of the bands of the uncleaved and cleaved ribozymes. To take account of the amount of labeled adenine residues contained in the cleaved and uncleaved RNAs, the single band intensities were divided by the number of adenine residues present in the relative RNA sequence. The kinetic traces were fitted using two different exponential functions in Origin 8.6G (see Results section for details).

In vivo assay: bulk fluorescence measurements

For the *in vivo* expression assays, the different clones were first pre-cultivated overnight aerobically at 37 °C on a LB agar Petri dishes supplemented with 100 μg per mL carbenicillin. The enhanced green fluorescent protein (eGFP) expression levels were evaluated performing bulk fluorescence measurements. 100 μL of each culture were transferred into 96-well-microplates and the OD_{600} and the fluorescence of the expressed eGFP (excitation wavelength = 488 nm, emission wavelength = 535 nm) were measured with a TECAN infinite M200 plate reader. The background value was determined measuring the fluorescence of an equally treated *E. coli* BL21(DE3) gold culture carrying a pET16b vector containing a truncated form of the eGFP gene. Fluorescence values were divided by the respective OD_{600} values and further analyzed. The fluorescence measurements for the *in vivo* assay were performed using a detector gain of 63. The error bars in the graphs represent the standard deviation calculated on independent biological quadruplicates. The correlation analysis was performed using R (https://www.r-project.org).

In vivo screening

For the screening of new communication modules from the combinatorial libraries, single clones of the transformed pool were picked into 96 deep well plates and let outgrown to stationary phase in 400 μL of LB medium supplemented with 100 μg per mL carbenicillin at 37 °C. 10 μL of bacterial culture were re-inoculated in fresh medium in the presence and in the absence of the specific ligands. The bacterial cultures were grown to stationary phase (19 hours) shaking vigorously at 37 °C. The screening of the theophylline-dependent switch library was performed in LB medium supplemented with 100 μg per mL carbenicillin in absence and in the presence of 2.5 mM theophylline (Fluka). The screenings of the TPP-dependent switch library was performed in M9 medium supplemented with 0.4% glucose and 100 μg per mL carbenicillin. The final concentration of thiamin (Fluka) was 1 mM. Bulk fluorescence of the cultures was measured using the protocol illustrated in the previous section to evaluate the differential expression of eGFP in the presence and in the absence of the respective ligand. The measurements were performed using a detector gain of 63 for the theophylline library or 65 for the TPP library. Clones that showed differential levels of eGFP expression in the presence and in the absence of the ligand were isolated and sequenced. Catalytically inactive mutants were also generated by site-direct mutagenesis. After the screening, a final validation was performed measuring the eGFP expression levels of the selected artificial riboswitches and the relative catalytically inactive controls. The error bars represent standard deviations calculated on biological triplicates.

Disclosure of potential conflicts of interest

No potential conflicts of interest were disclosed.

Funding

Financial support by the Graduate School Chemical Biology (KoRS-CB) and the German Research Foundation (DFG) within the SFB 969 is acknowledged. Funding for open access charges: University of Konstanz.

References

1. Picard F, Milhem H, Loubiere P, Laurent B, Cocaign-Bousquet M, Girbal L. Bacterial translational regulations: high diversity between all mRNAs and major role in gene expression. BMC Genomics. 2012;13:528. doi:10.1186/1471-2164-13-528.
2. Del Campo C, Bartholomaus A, Fedyunin I, Ignatova Z. Secondary structure across the bacterial transcriptome reveals versatile roles in mRNA regulation and function. PLoS Genet. 2015;11:e1005613. doi:10.1371/journal.pgen.1005613.
3. von Hippel PH. An integrated model of the transcription complex in elongation, termination, and editing. Science. 1998;281:660–5. doi:10.1126/science.281.5377.660.
4. Lesnik EA, Sampath R, Levene HB, Henderson TJ, McNeil JA, Ecker DJ. Prediction of rho-independent transcriptional terminators in Escherichia coli. Nucleic Acids Res. 2001;29:3583–94. doi:10.1093/nar/29.17.3583.
5. Landick R. RNA polymerase slides home: pause and termination site recognition. Cell. 1997;88:741–4. doi:10.1016/S0092-8674(00)81919-4.
6. Martin FH, Tinoco I, Jr. DNA-RNA hybrid duplexes containing oligo (dA:rU) sequences are exceptionally unstable and may facilitate termination of transcription. Nucleic Acids Res. 1980;8:2295–9. doi:10.1093/nar/8.10.2295.

7. Laalami S, Zig L, Putzer H. Initiation of mRNA decay in bacteria. Cell Mol Life Sci. 2014;71:1799–828. doi:10.1007/s00018-013-1472-4.
8. Mott JE, Galloway JL, Platt T. Maturation of Escherichia coli tryptophan operon mRNA: evidence for 3′ exonucleolytic processing after rho-dependent termination. EMBO J. 1985;4:1887–91.
9. Regnier P, Hajnsdorf E. Poly(A)-assisted RNA decay and modulators of RNA stability. Prog Mol Biol Transl Sci. 2009;85:137–85. doi:10.1016/S0079-6603(08)00804-0.
10. Mohanty BK, Kushner SR. Bacterial/archaeal/organellar polyadenylation. Wiley Interdiscip Rev RNA. 2011;2:256–76. doi:10.1002/wrna.51.
11. Blum E, Carpousis AJ, Higgins CF. Polyadenylation promotes degradation of 3′-structured RNA by the Escherichia coli mRNA degradosome in vitro. J Biol Chem. 1999;274:4009–16. doi:10.1074/jbc.274.7.4009.
12. Smolke CD, Carrier TA, Keasling JD. Coordinated, differential expression of two genes through directed mRNA cleavage and stabilization by secondary structures. Appl Environ Microbiol. 2000;66:5399–405. doi:10.1128/AEM.66.12.5399-5405.2000.
13. Smolke CD, Keasling JD. Effect of copy number and mRNA processing and stabilization on transcript and protein levels from an engineered dual-gene operon. Biotechnol Bioeng. 2002;78:412–24. doi:10.1002/bit.10218.
14. Smolke CD, Keasling JD. Effect of gene location, mRNA secondary structures, and RNase sites on expression of two genes in an engineered operon. Biotechnol Bioeng. 2002;80:762–76. doi:10.1002/bit.10434.
15. Newbury SF, Smith NH, Higgins CF. Differential mRNA stability controls relative gene expression within a polycistronic operon. Cell. 1987;51:1131–43. doi:10.1016/0092-8674(87)90599-X.
16. Opdyke JA, Fozo EM, Hemm MR, Storz G. RNase III participates in GadY-dependent cleavage of the gadX-gadW mRNA. J Mol Biol. 2011;406:29–43. doi:10.1016/j.jmb.2010.12.009.
17. Chao Y, Papenfort K, Reinhardt R, Sharma CM, Vogel J. An atlas of Hfq-bound transcripts reveals 3′ UTRs as a genomic reservoir of regulatory small RNAs. EMBO J. 2012;31:4005–19. doi:10.1038/emboj.2012.229.
18. Perreault J, Weinberg Z, Roth A, Popescu O, Chartrand P, Ferbeyre G, Breaker RR. Identification of hammerhead ribozymes in all domains of life reveals novel structural variations. PLoS Comput Biol. 2011;7:e1002031. doi:10.1371/journal.pcbi.1002031.
19. Hammann C, Luptak A, Perreault J, de la Pena M. The ubiquitous hammerhead ribozyme. RNA. 2012;18:871–85. doi:10.1261/rna.031401.111.
20. de la Pena M, Garcia-Robles I. Ubiquitous presence of the hammerhead ribozyme motif along the tree of life. RNA. 2010;16:1943–50. doi:10.1261/rna.2130310.
21. Roth A, Weinberg Z, Chen AG, Kim PB, Ames TD, Breaker RR. A widespread self-cleaving ribozyme class is revealed by bioinformatics. Nat Chem Biol. 2014;10:56–60. doi:10.1038/nchembio.1386.
22. Weinberg Z, Kim PB, Chen TH, Li S, Harris KA, Lunse CE, Breaker RR. New classes of self-cleaving ribozymes revealed by comparative genomics analysis. Nat Chem Biol. 2015;11:606–10. doi:10.1038/nchembio.1846.
23. Felletti M, Stifel J, Wurmthaler LA, Geiger S, Hartig JS. Twister ribozymes as highly versatile expression platforms for artificial riboswitches. Nat Commun. 2016;7:12834. doi:10.1038/ncomms12834.
24. Feng X, Liu L, Duan X, Wang S. An engineered riboswitch as a potential gene-regulatory platform for reducing antibacterial drug resistance. Chem Commun (Camb) 2011;47:173–5. doi:10.1039/C0CC00980F.
25. Wilson TJ, Liu Y, Domnick C, Kath-Schorr S, Lilley DM. The Novel Chemical Mechanism of the Twister Ribozyme. J Am Chem Soc. 2016;138:6151–62. doi:10.1021/jacs.5b11791.
26. Webb CH, Riccitelli NJ, Ruminski DJ, Luptak A. Widespread occurrence of self-cleaving ribozymes. Science. 2009;326:953. doi:10.1126/science.1178084.
27. Garcia-Robles I, Sanchez-Navarro J, de la Pena M. Intronic hammerhead ribozymes in mRNA biogenesis. Biol Chem. 2012;393:1317–26. doi:10.1515/hsz-2012-0223.
28. Laha T, McManus DP, Loukas A, Brindley PJ. Sjalpha elements, short interspersed element-like retroposons bearing a hammerhead ribozyme motif from the genome of the oriental blood fluke Schistosoma japonicum. Biochim Biophys Acta. 2000;1492:477–82. doi:10.1016/S0167-4781(00)00112-3.
29. Cervera A, Urbina D, de la Pena M. Retrozymes are a unique family of non-autonomous retrotransposons with hammerhead ribozymes that propagate in plants through circular RNAs. Genome Biol. 2016;17:135. doi:10.1186/s13059-016-1002-4.
30. Kolev NG, Hartland EI, Huber PW. A manganese-dependent ribozyme in the 3′-untranslated region of Xenopus Vg1 mRNA. Nucleic Acids Res. 2008;36:5530–9. doi:10.1093/nar/gkn530.
31. Fürtig B, Richter C, Schell P, Wenter P, Pitsch S, Schwalbe H. NMR-spectroscopic characterization of phosphodiester bond cleavage catalyzed by the minimal hammerhead ribozyme. RNA Biol. 2008;5:41–8. doi:10.4161/rna.5.1.5704.
32. Bernstein JA, Khodursky AB, Lin PH, Lin-Chao S, Cohen SN. Global analysis of mRNA decay and abundance in Escherichia coli at single-gene resolution using two-color fluorescent DNA microarrays. Proc Natl Acad Sci U S A. 2002;99:9697–702. doi:10.1073/pnas.112318199.
33. Selinger DW, Saxena RM, Cheung KJ, Church GM, Rosenow C. Global RNA half-life analysis in Escherichia coli reveals positional patterns of transcript degradation. Genome Res. 2003;13:216–23. doi:10.1101/gr.912603.
34. Arraiano CM, Mauxion F, Viegas SC, Matos RG, Seraphin B. Intracellular ribonucleases involved in transcript processing and decay: precision tools for RNA. Biochim Biophys Acta. 2013;1829:491–513. doi:10.1016/j.bbagrm.2013.03.009.
35. Agop-Nersesian C, Pfahler J, Lanzer M, Meissner M. Functional expression of ribozymes in Apicomplexa: towards exogenous control of gene expression by inducible RNA-cleavage. Int J Parasitol. 2008;38:673–81. doi:10.1016/j.ijpara.2007.10.015.
36. Folichon M, Marujo PE, Arluison V, Le Derout J, Pellegrini O, Hajnsdorf E, Régnier P. Fate of mRNA extremities generated by intrinsic termination: detailed analysis of reactions catalyzed by ribonuclease II and poly(A) polymerase. Biochimie. 2005;87:819–26. doi:10.1016/j.biochi.2005.02.012.
37. Yehudai-Resheff S, Schuster G. Characterization of the E.coli poly(A) polymerase: nucleotide specificity, RNA-binding affinities and RNA structure dependence. Nucleic Acids Res. 2000;28:1139–44. doi:10.1093/nar/28.5.1139.
38. Andrade JM, Hajnsdorf E, Regnier P, Arraiano CM. The poly(A)-dependent degradation pathway of rpsO mRNA is primarily mediated by RNase R. RNA. 2009;15:316–26. doi:10.1261/rna.1197309.
39. Vinkenborg JL, Karnowski N, Famulok M. Aptamers for allosteric regulation. Nat Chem Biol. 2011;7:519–27. doi:10.1038/nchembio.609.
40. Haller A, Altman RB, Souliere MF, Blanchard SC, Micura R. Folding and ligand recognition of the TPP riboswitch aptamer at single-molecule resolution. Proc Natl Acad Sci U S A. 2013;110:4188–93. doi:10.1073/pnas.1218062110.
41. Qi L, Haurwitz RE, Shao W, Doudna JA, Arkin AP. RNA processing enables predictable programming of gene expression. Nat Biotechnol. 2012;30:1002–6. doi:10.1038/nbt.2355.
42. Gautheret D, Lambert A. Direct RNA motif definition and identification from multiple sequence alignments using secondary structure profiles. J Mol Biol. 2001;313:1003–11. doi:10.1006/jmbi.2001.5102.
43. Macke TJ, Ecker DJ, Gutell RR, Gautheret D, Case DA, Sampath R. RNAMotif, an RNA secondary structure definition and search algorithm. Nucleic Acids Res. 2001;29:4724–35. doi:10.1093/nar/29.22.4724.